CHECKERBOARD-FREE TOPOLOGY OPTIMIZATION USING POLYGONAL FINITE ELEMENTS

Anderson Pereira[a], Cameron Talischi[b], Ivan F. M. Menezes[a] and Glaucio H. Paulino[b]

[a]*Tecgraf (Group of Technology in Computer Graphics), Pontifical Catholic University of Rio de Janeiro (PUC–Rio), Rua Marquês de São Vicente, 225, 22453-900, Rio de Janeiro, RJ, Brazil, {anderson,ivan}@tecgraf.puc-rio.br, http://www.tecgraf.puc-rio.br*

[b]*Department of Civil and Environmental Engineering, University of Illinois at Urbana-Champaign, Newmark Laboratory, 205 North Mathews Avenue, Urbana, IL, 61801, U.S.A. {ktalisch,paulino}@uiuc.edu, http://cee.illinois.edu*

Keywords: topology optimization, polygonal elements, Voronoi tessellations

Abstract. The checkerboard layout of material distribution is one of a number of serious numerical anomalies encountered in the solution of topology optimization problems. Regularization schemes such as filtering can be used to suppress the numerical instabilities, but these measures often involve heuristic parameters that can augment the optimization problem. Polygonal elements can be very useful in this aspect since they naturally exclude checkerboard layouts and provide flexibility in discretizing complex domains. Examples considering compliance minimization and compliant mechanism are presented that demonstrate the advantages of the proposed elements in achieving checkerboard-free solutions and avoiding one-node connections from the design optimization process. Potential extensions and impact of this work will also be discussed.

1 INTRODUCTION

The main focus of this work is the numerical instabilities that plague the finite element solutions to the topology optimization problems. The appearance of such spurious solution is attributed to the poor modeling of the response field (displacements in structural optimization applications) stemming from an inappropriate choice of finite element discretizations. The formation of the so-called checkerboard patterns, for example, has been attributed to the artificially high stiffness of lower order quad or triangular elements (Diaz and Sigmund, 1995; Jog and Haber, 1996). The alternating void-solid checkerboard patterns avoid penalization imposed on the intermediate densities and are therefore favored in compliance minimization and compliant mechanism problems. It has been previously observed that higher order elements (Sigmund and Petersson, 1998) and non-conforming elements (Jang et al., 2003) are less susceptible to the appearance of such solutions.

In Talischi et al. (2009), it was noted that the discretization of the density field also plays a role in the appearance of checkerboard patterns. The exclusion of one-one connections in a hexagonal mesh naturally excludes such designs. In the extension of that work (Talischi et al., 2010), it was shown that general convex polygonal discretizations also enjoy numerical stability. Additionally, they provide more flexibility in mesh generation and impose less constraint in the formation of optimal designs, which as a result are less mesh-dependent.

In the present work, we continue our investigation of the use of polygonal discretizations in structural topology optimization applications. We present benchmark compliance minimization and compliant mechanism problems and compare the performance of polygonal element to standard bilinear elements.

2 FORMULATIONS

The discrete form of the problem is mathematically given by:

$$\begin{aligned} \min_{\rho} \quad & J\left(\rho, \mathbf{u}\right) \\ \text{s.t.:} \quad & \mathbf{K}(\rho)\mathbf{u} = \mathbf{f} \\ & \int_{\Omega_S} dV \leq V_s \end{aligned} \tag{1}$$

Here $J\left(\rho, \mathbf{u}\right)$ is the cost function that characterizes the performance of each design; $\mathbf{f}$ and $\mathbf{u}$ are the global force and displacement vectors; $\mathbf{K}$ denotes the global stiffness matrix, which is dependent on the design variable ρ; and V_s is the upper bound on the volume of the design denoted by Ω_S.

The minimum compliance problem is given by:

$$J\left(\rho, \mathbf{u}\right) = \mathbf{f}^T\mathbf{u} \tag{2}$$

while for the compliant mechanism, we have:

$$J\left(\rho, \mathbf{u}\right) = \mathbf{l}^T\mathbf{u} \tag{3}$$

where $\mathbf{l}$ is a vector composed of zeros except the degree of the output position which is one.

The common choice of design parametrization is to take ρ as the material "density": by convention, $\rho = 1$ at a point signifies a material region while $\rho = 0$ represents void. The

intermediate values are penalized according to the following scheme:

$$E(\rho) = \rho^p E^0, \quad p > 1 \tag{4}$$

Here $E(\rho)$ is the material stiffness of a point with density ρ, while E^0 denotes the stiffness of the solid phase (corresponding to $\rho = 1$). For values of p greater than 1 (usually we take $p \geq 3$), the stiffness of intermediate densities is penalized through the power law relation, so they are not favored. As a result, the final design consists primarily of solid and void regions. This approach is known as the Solid Isotropic Material with Penalization (SIMP), and readers are referred to Bendsøe (1989); Zhou and Rozvany (1991); Bendsøe and Sigmund (2003) for more information.

We have considered the following discretizations of the density field: (1) Element-based (2) Projection scheme.

2.1 Element-based approach:

In this approach, a constant density value is assigned to each displacement finite element. These element densities ρ_e are then used as the design variables for the optimization problem (1). It is in this context that the checkerboard appears: the density of adjacent elements alternates between zero and one, while the patch of element maintains the connectivity resembling that of a checkerboard.

For the present formulation, as mentioned before, convex polygonal elements are used to construct the finite element discretization. Therefore, the element-based approach with such a discretization does not favor spurious checkerboard-like patterns. Furthermore, polygonal meshes can remove the restrictions on the orientation of the structural members and the final topology as arbitrary polygonal elements have less directional bias when compared to quadrilateral elements. For example, hexagonal element has more lines of symmetry per element compared to the triangular and square elements.

The polygonal finite element mesh can be constructed using a Voronoi diagram of the nodes that cover the design domain.

The interpolation space on the polygonal mesh is constructed using Laplace (natural neighbor) shape functions as described in Sukumar and Malsch (2006); Sukumar and Tabarraei (2004). These shape functions yield a conforming finite element, and satisfy the necessary approximability conditions of constant and linear precision, and exhibit desirable properties such as partition of unity. Moreover, they provide an isoparametric transformation map that allows the computations to be carried out on a parent element. For more details on the implementation of these elements, we refer the reader to the references mentioned above.

2.2 Projection scheme:

In this approach (Guest et al., 2004), the density of each element is obtained by a weighted average of the values of the design variables in the adjacent elements. In particular, the projection is carried out as:

$$\rho_e = \frac{\sum_i w_i d_i}{\sum_i w_i} \tag{5}$$

As before, ρ_e is the element density; d_i is the design variable associated to element i, and w_i are

the weighting functions defined by:

$$w_i = \max\left(\frac{r_{min} - r_i}{r_{min}}, 0\right) \tag{6}$$

Here r_i is the distance between the centroid of element i to the centroid of element e, and r_{min} is a prescribed radius of projection. We can see that the projection has an embedded physical length scale r_{min} that is independent of the mesh size. As such, this scheme addresses the issue of mesh-dependency in topology optimization by limiting the space of admissible solutions to the design having members larger than a minimum physical size.

3 NUMERICAL RESULTS

In this section, numerical results are presented to confirm the checkerboard-free design by using polygonal elements. Both compliance minimization and compliant mechanism are considered. The optimization problem is solved using the Optimality Criteria (OC) developed by Bendsøe and Sigmund (2003). Also, to avoid getting trapped at a local minima, a continuation method is used on the value of SIMP penalty exponent: p is increased (with increment of 0.5) from 1 to 3 after the maximum change in the design variables is less than a given tolerance of 0.01. The maximum number of iterations per value of p used was 100.

3.1 Compliance minimization example

In this section, the numerical results for the cantilever beam problem are presented (see Figure 1). The Poisson's ratio is taken as 0.3 and the volume fraction V_s is 50% of the volume of the extended design domain.

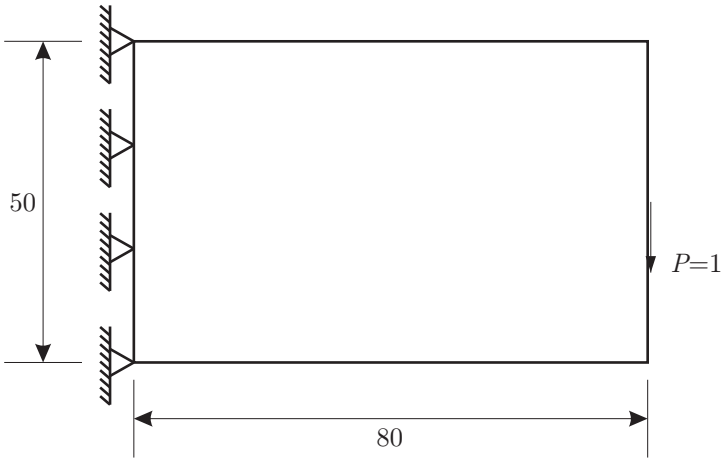

Figure 1: Cantilever beam domain.

In Figure 2, the results of the element-based formulation for the Q4 element and the polygonal element are shown. The solutions with Q4 implementation contain patches of checkerboard while no such fine scale patterns are observed with the polygonal implementation. Note that no filtering technique or density gradient was imposed and thus the checkerboard-free property of the polygonal element is attributed essentially to its geometric features and interpolation characteristics. We should emphasize that the checkerboard solutions are unphysical and do not correspond to the optimal structure.

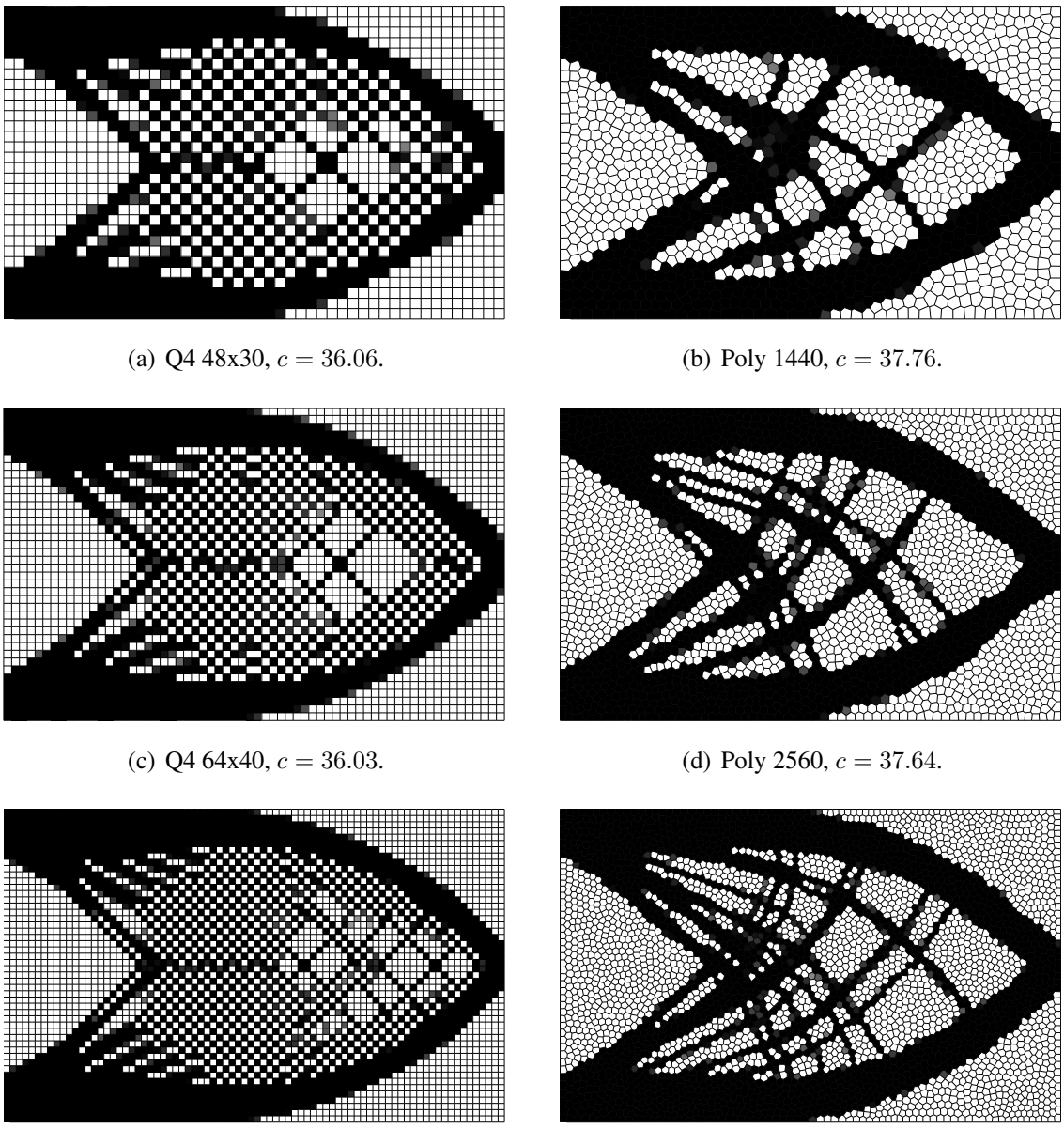

(a) Q4 48x30, $c = 36.06$.

(b) Poly 1440, $c = 37.76$.

(c) Q4 64x40, $c = 36.03$.

(d) Poly 2560, $c = 37.64$.

(e) Q4 80x50, $c = 36.03$.

(f) Poly 4000, $c = 37.79$.

Figure 2: Cantilever beam design with element–based formulation.

The results using projection scheme are presented in Figure 3. The radius of the projection r_{min} is taken to be 7.5% of the height of the beam and independent of the mesh size. The length scale imposed on the optimization through r_{min} guarantees mesh-independent solutions that satisfy the required minimum member size.

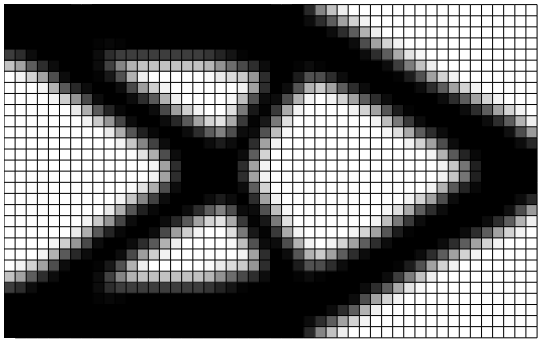

(a) Q4 48x30, $c = 42.53$.

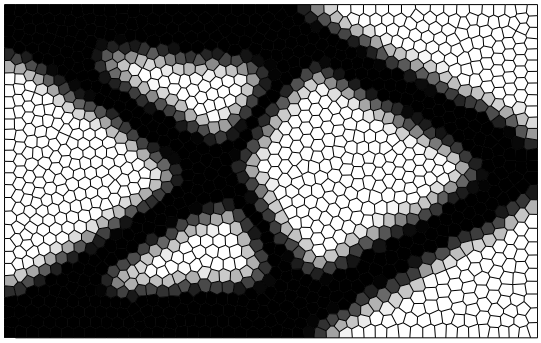

(b) Poly 1440, $c = 42.40$.

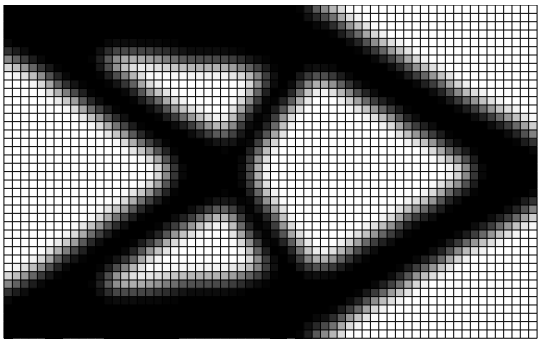

(c) Q4 64x40, $c = 42.89$.

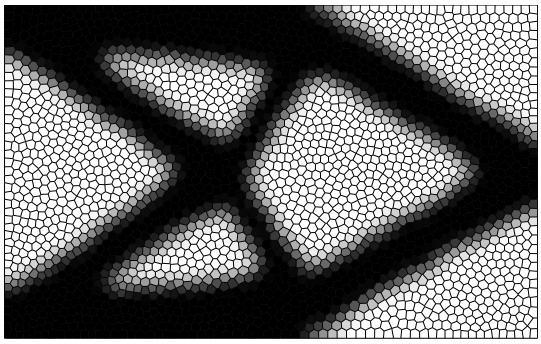

(d) Poly 2560, $c = 42.86$.

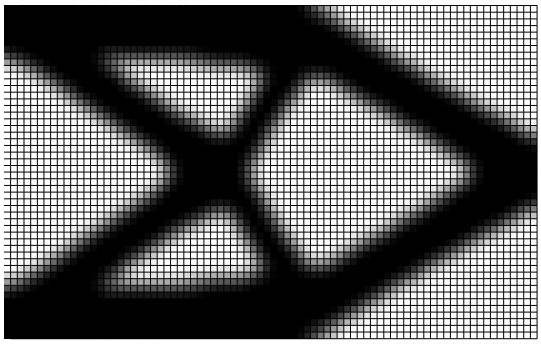

(e) Q4 80x50, $c = 42.73$.

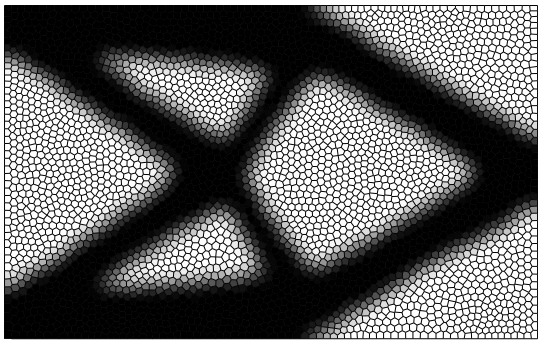

(f) Poly 4000, $c = 42.97$.

Figure 3: Cantilever beam design with projection method formulation.

3.2 Compliant mechanism example

The numerical results for the force inverter compliant mechanism design problem, depicted in Figure 4(a), are presented (Bendsøe and Sigmund, 2003). Due to the symmetry of the problem, only half of the domain is considered in the optimization algorithm (see Figure 4(b)). The Poisson's ratio is taken as 0.3 and the volume fraction V_s is 30% of the volume of the extended design domain. The springs k_1 and k_2 are 0.1.

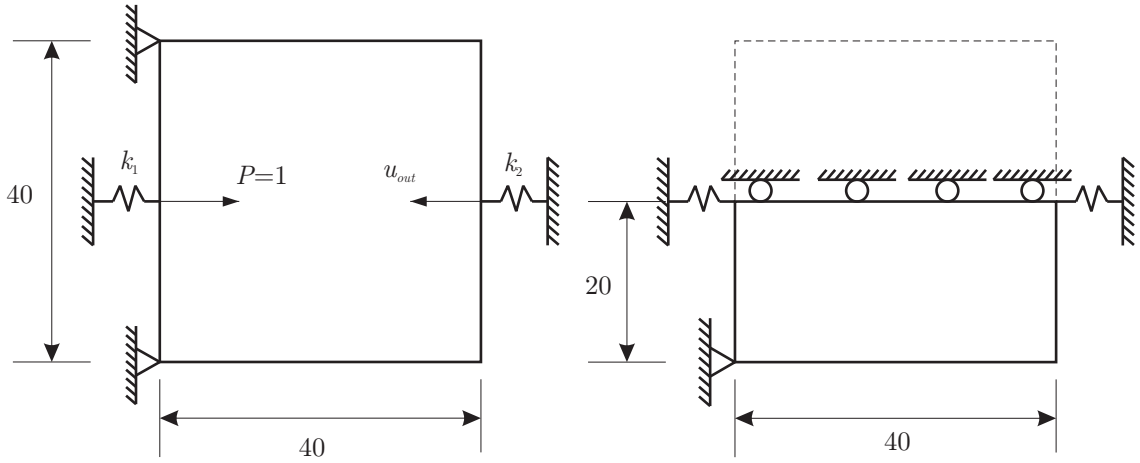

(a) Full domain. (b) Half domain.

Figure 4: Inverter mechanism domain.

The parameters used here in the OC-method are the ones proposed by Bendsøe and Sigmund (2003), i.e., for the move limit we use $\delta = 0.1$, and for the "numerical damping parameter" we use $\eta = 0.3$. Also, we use the following expression:

$$\frac{\mathrm{d}J^k}{\mathrm{d}d_i} = \min\left(-\epsilon_c, \frac{\mathrm{d}J^k}{\mathrm{d}d_i}\right); \qquad \epsilon_c > 0 \tag{7}$$

proposed by Bendsøe and Sigmund (2003), where $\epsilon_c = 1 \times 10^{-10}$.

The results of the element-based formulation for the Q4 element and the polygonal element are shown in Figure 5. As in the previous example, the solutions with Q4 implementation contain patches of checkerboard while no such fine scale patterns are observed with the polygonal implementation.

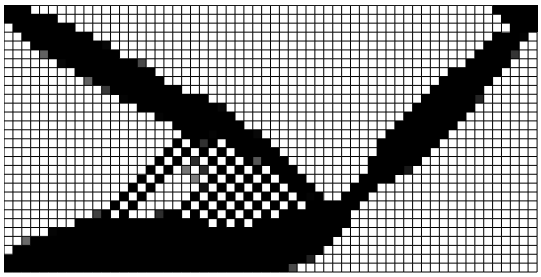

(a) Q4 60x30, $u_{out} = -1.089$.

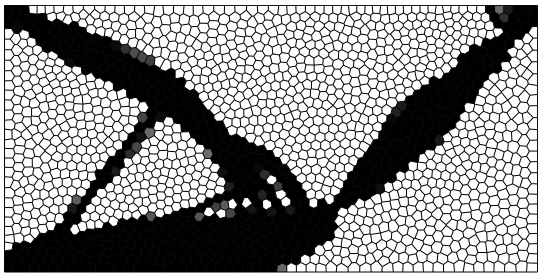

(b) Poly 1800, $u_{out} = -1.088$.

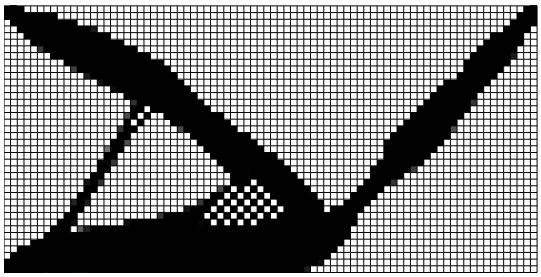

(c) Q4 80x40, $u_{out} = -1.041$.

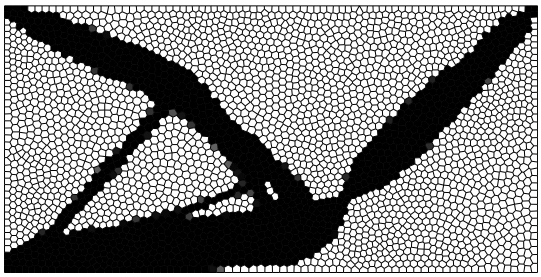

(d) Poly 3200, $u_{out} = -1.104$.

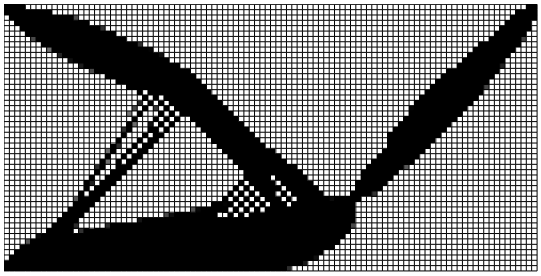

(e) Q4 100x50, $u_{out} = -1.057$.

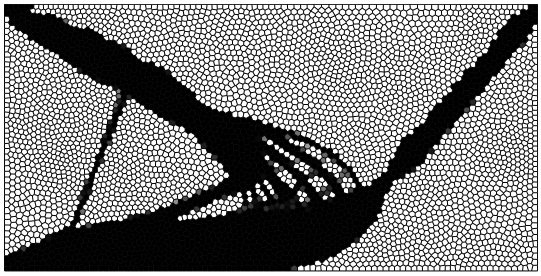

(f) Poly 5000, $u_{out} = -0.930$.

Figure 5: Inverter mechanism design with element–based formulation.

The results using projection scheme are presented in Figure 6. The radius of the projection r_{min} is taken to be 6% of the height.

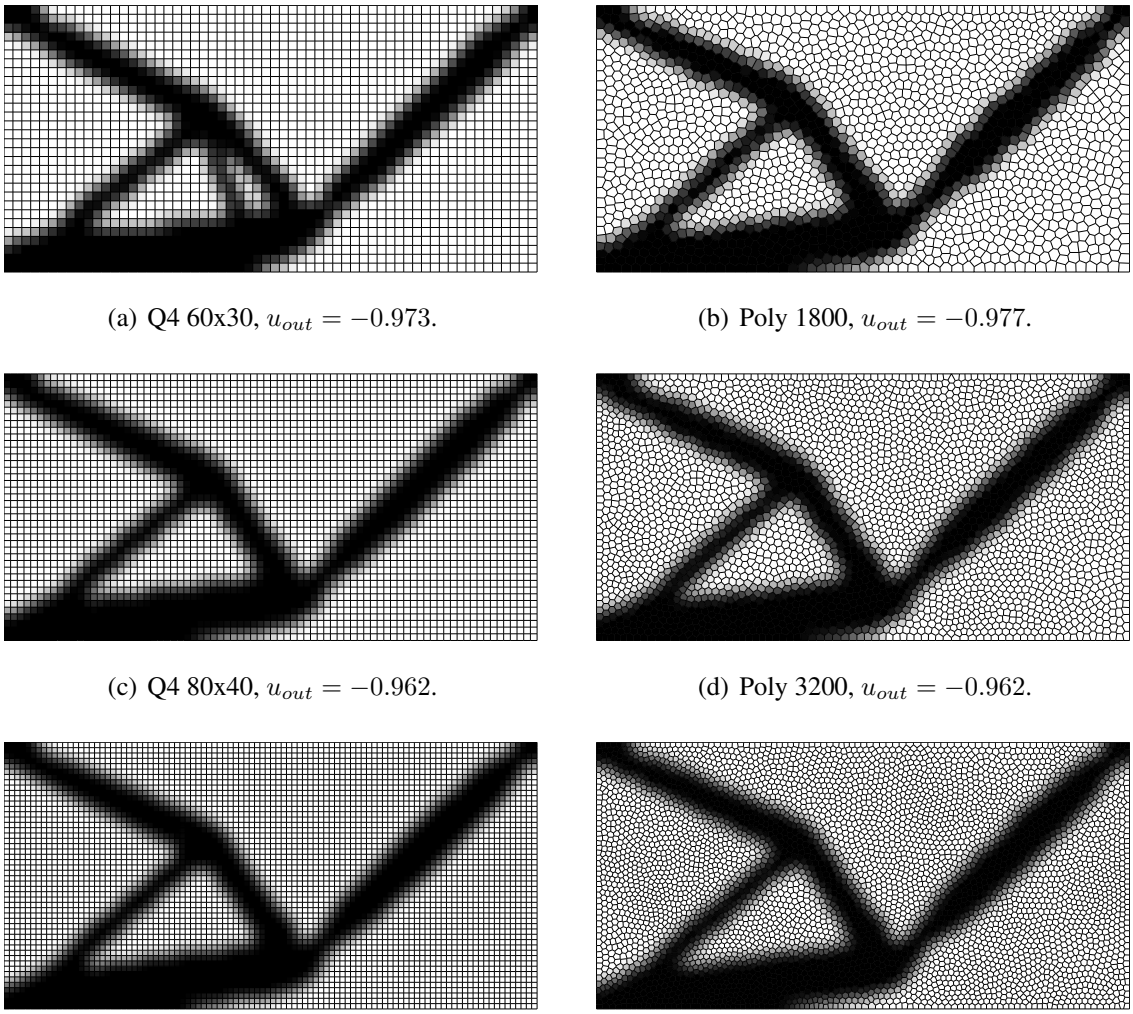

(a) Q4 60x30, $u_{out} = -0.973$.

(b) Poly 1800, $u_{out} = -0.977$.

(c) Q4 80x40, $u_{out} = -0.962$.

(d) Poly 3200, $u_{out} = -0.962$.

(e) Q4 100x50, $u_{out} = -0.953$.

(f) Poly 5000, $u_{out} = -0.939$.

Figure 6: Inverter mechanism design with projection method formulation.

4 CONCLUSIONS

In this work, the checkerboard pathology in topology optimization is addressed and the use of polygonal finite elements is proposed. As discussed and demonstrated by means of the presented numerical examples, the use of such elements eliminates the formation of checkerboard and provides a robust and stable means for solving topology optimization problems. Extensions to the present work that consider the use of the Level Set Method (Osher and Fedkiw, 2003) is currently under investigation by the authors.

ACKNOWLEDGEMENTS

The authors Anderson Pereira and Ivan Menezes acknowledge the financial support provided by Tecgraf (Group of Technology in Computer Graphics), PUC-Rio, Rio de Janeiro, Brazil. Cameron Talischi and Glaucio Paulino acknowledge the support by the Department of Energy Computational Science Graduate Fellowship Program of the Office of Science and National Nuclear Security Administration in the Department of Energy under contract DE-FG02-97ER25308.

REFERENCES

Bendsøe M. Optimal shape design as a material distribution problem. *Structural Optimization*, 1(4):193–202, 1989.

Bendsøe M. and Sigmund O. *Topology Optimization Theory, Methods and Applications*. Berlin: Springer, 2003.

Diaz A. and Sigmund O. Checkerboard patterns in layout optimization. *Structural Optimization*, 10:40–45, 1995.

Guest J., Prevost J., and Belytschko T. Achieving minimum length scale in topology optimization using nodal design variables and projection functions. *International Journal for Numerical Methods in Engineering*, 61(2):238–254, 2004.

Jang G., Jeong H., Kim Y., Sheen D., Park C., and Kim M. Checkerboard-free topology optimization using non–conforming finite elements. *International Journal for Numerical Methods in Engineering*, 57(12):1717–1735, 2003.

Jog C. and Haber R. Stability of finite element models for distributed-parameter optimization and topology design. *Computer Methods in Applied Mechanics and Engineering*, 130:203–226, 1996.

Osher S. and Fedkiw R. *Level Set Methods and Dynamic Implicit Surfaces*. Springer–Verlag, New York, 2003.

Sigmund O. and Petersson J. Numerical instabilities in topology optimization: A survey on procedures dealing with checkerboard, mesh-dependence and local minima. *Structural Optimization*, 16:68–75, 1998.

Sukumar N. and Malsch E. Recent advances in the construction of polygonal finite element interpolants. *Archives of Computational Methods in Engineering*, 13(1):129–163, 2006.

Sukumar N. and Tabarraei A. Conforming polygonal finite elements. *International Journal for Numerical Methods in Engineering*, 61:2045–2066, 2004.

Talischi C., Paulino G.H., and Le C. Honeycomb wachspress finite elements for structural topology optimization. *Structural and Multidisciplinary Optimization*, 37(6):569–583, 2009.

Talischi C., Paulino G.H., Pereira A., and Menezes I.F.M. Polygonal finite elements for topology optimization: A unifying paradigm. *International Journal for Numerical Methods in Engineering*, 82(6):671–698, 2010.

Zhou M. and Rozvany G. The COC algorithm, Part II: Topological, geometry and generalized shape optimization. *Computer Methods in Applied Mechanics and Engineering*, 89:197–224, 1991.